Supplemental Figure 1

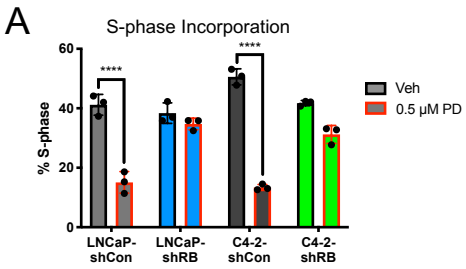

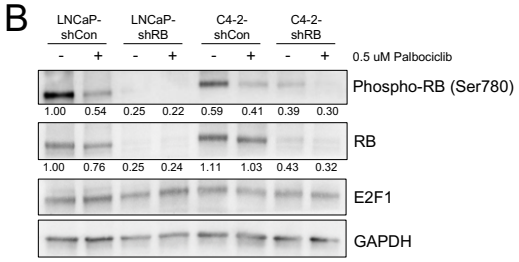

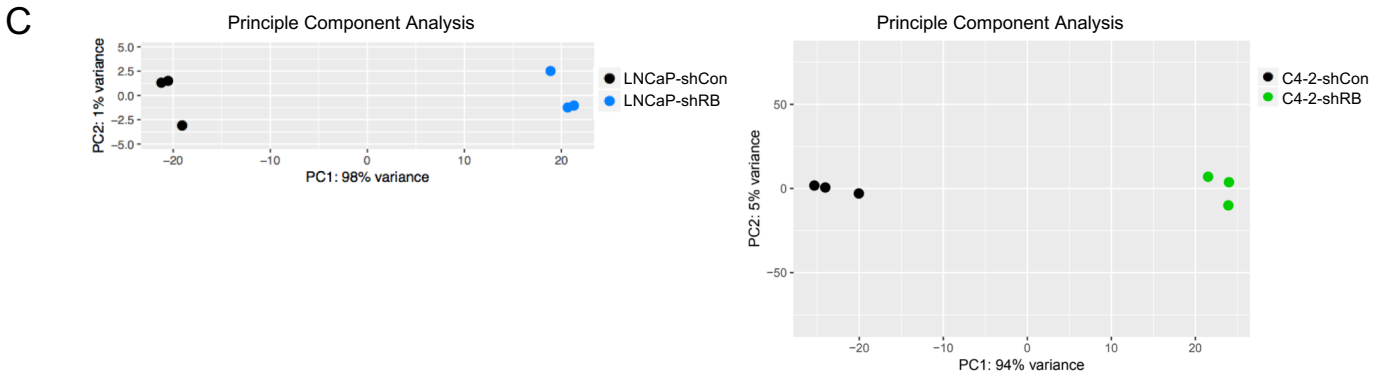

Supplemental Figure 1. RB depletion in functionally intact HSPC and CRPC models results in differential gene regulation. (A) Cell cycle progression was measured by S-phase incorporation in HSPC and CRPC isogenic models following treatment with 0.5 μM Palbociblib (PD) for 24 hours. S-phase incorporation as significantly reduced in HSPC and CRPC control models following PD treatment. (B) Protein expression of phosphorylated RB, total RB, and E2F1 was examined with and without treatment with 0.5 μM PD for 24 hours. Phospho-RB was reduced following treatment with PD. (C) Principle Component Analysis for LNCaP-shCon, LNCaP-shRB (Left) and C4-2-shCon, C4-2-shRB (right) RNA-seq.

Supplemental Figure 2

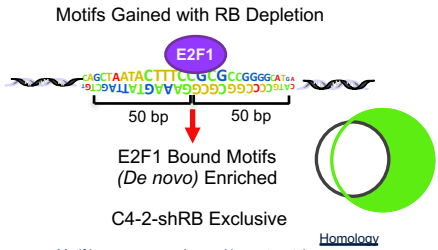

Motif logo	p-value	Nearest match	Homology score
	1.00E-1399	BORIS	0.923
	1.00E-272	FOXM1	0.972
	1.00E-106	NF1-halfsite	0.956
	1.00E-60	MAX	0.696
	1.00E-55	GRE(NR)	0.703
	1.00E-55	E2F6	0.952
	1.00E-46	Sox15	0.638
	1.00E-38	FOS	0.785
	1.00E-37	Foxa2	0.764
	1.00E-36	Tlx?(NR)	0.860
	1.00E-35	GRHL1	0.789
	1.00E-35	Osr2	0.665
	1.00E-30	Unknown (Homeobox)	0.842
	1.00E-30	NFATC1	0.701
	1.00E-23	Ets1	0.689
	1.00E-21	Rhox11	0.625
	1.00 E-21	Arnt1	0.845
	1.00E-20	SP1	0.841
	1.00E-20	HIF-1b	0.818

Supplemental Figure 2. E2F1 binding motifs expand upon RB1 depletion. Total list of *de novo* binding motifs exclusive to the RB1 depleted condition post CRPC. P-value < $1x10^{-20}$ and homology scores are shown.

Supplemental Figure 3

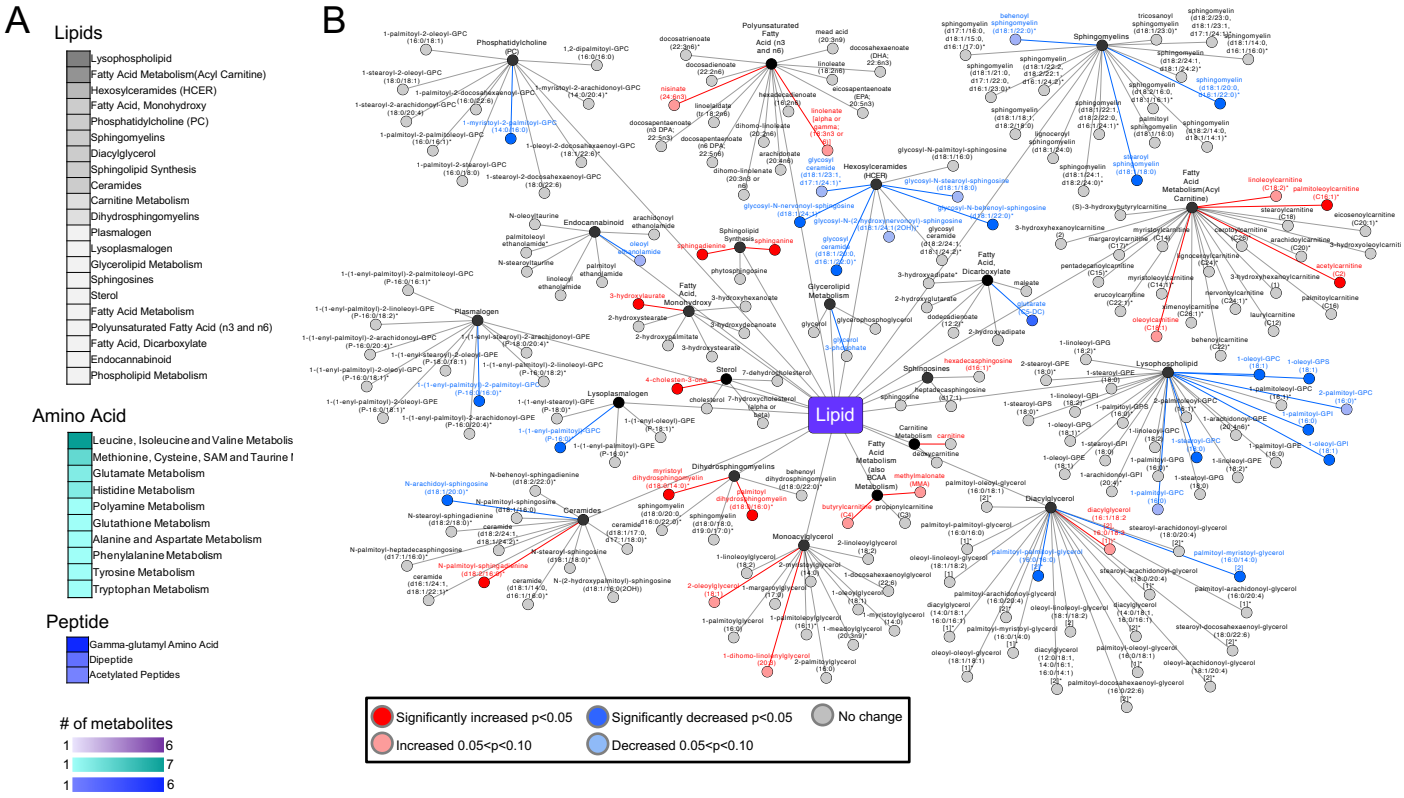

Supplemental Figure 3. RB loss drives altered lipid and peptide metabolism in castrate resistant models. (A) KEGG pathway analysis was performed and sub-pathways were identified within super altered metabolic pathways, the top three altered super pathways and sub-pathways are shown. (B) Map of lipid metabolism metabolites altered. Altered metabolites are shown in red (increased) and blue (decreased). Significant metabolites defined by p<0.05.

Supplemental Figure 4

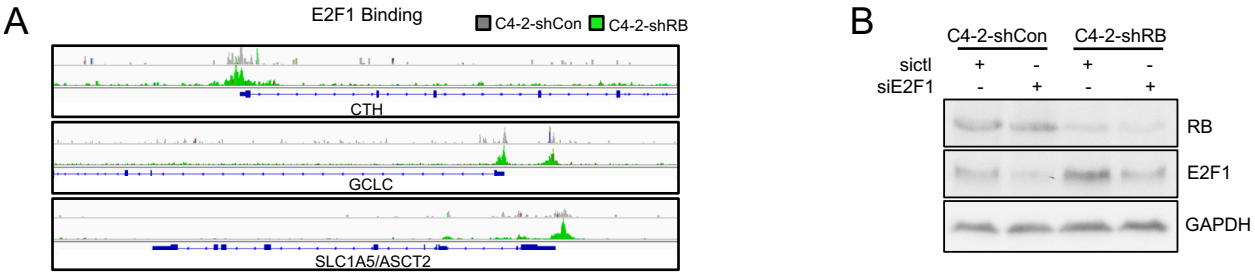

Supplemental Figure 4. RB1 depletion rewires E2F1 function to regulate glutathione metabolism. (A) E2F1 binding peaks in C4-2-shCon and C4-2-shRB models at select gene promoters involved in glutathione metabolism. **(B)** Western blot displaying RB and E2F1 knockdown in C4-2-shCon and C4-2-shRB models.

Supplemental Figure 5

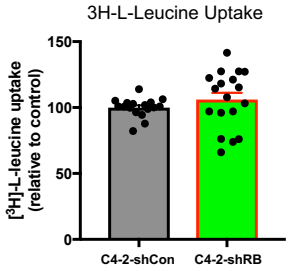

Supplemental Figure 5. RB depletion protects against ROS through increased glutathione synthesis. Leucine uptake assay in C4-2-shCon and C4-2-shRB models.

Supplemental Figure 6

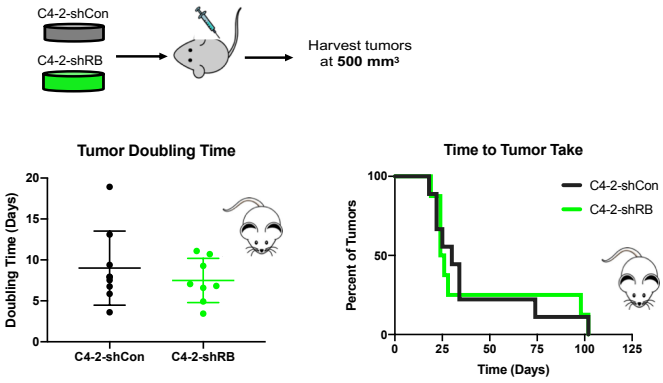

Supplemental Figure 6. RB1 depletion does not affect tumor growth *in vivo*. C4-2-shCon or C4-2-shRB cells were subcutaneously injected into both flanks of athymic nude mice. Tumors were harvested at 500 mm^3 tumor doubling time and time to tumor take was calculated.

Supplemental Figure 7

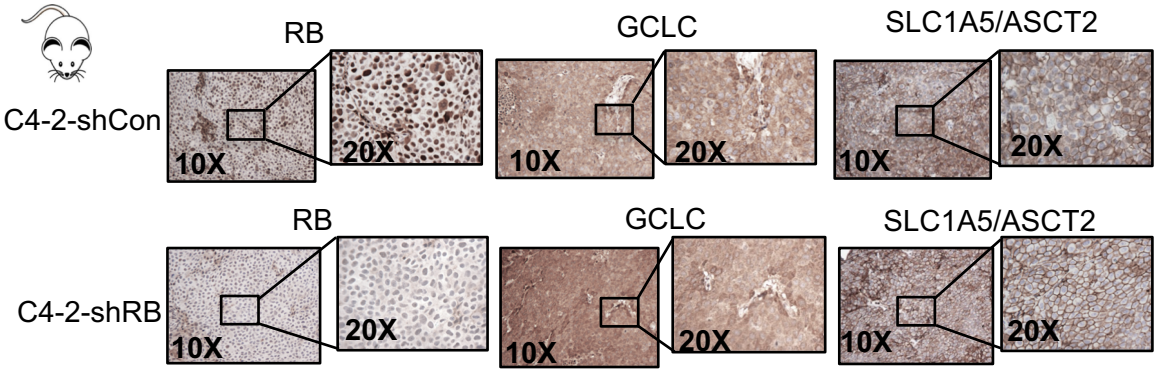

Supplemental Figure 7. RB1 depletion drives increased expression of proteins required for glutathione metabolism *in vivo.* Immunohistochemistry staining of target genes from tumor xenografts. C42-shCon or C42-shRB cells were subcutaneously injected into both flanks of athymic nude mice. Tumors were harvested at 500 mm^3 and sectioned for protein analysis. Tumor images at 10X and 40X are shown.

Supplemental Figure 8

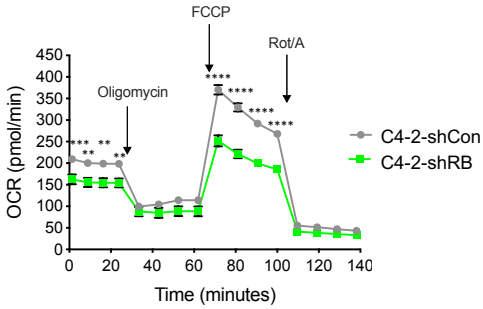

Supplemental Figure 8. RB1 depletion reduces mitochondrial function. Oxygen consumption rate (OCR) was measured in C42-shCon and C42-shRB cells using a Mito Stress Test kit on a Seahorse XF96e analyzer. OCR was decreased in RB depleted models compared to RB intact controls. Data are mean ± SEM, n=3 exps (4 technical replicates each); Two-way ANOVA test with Sidak's multiple comparisons test was performed using Prism 9.0. **, $P < 0.01$; ***, $P < 0.001$; ****, $P < 0.0001$.